A Comparison of Consistent Discretizations for Elliptic Problems on Polyhedral Grids

Øystein S. Klemetsdal, Olav Møyner, Xavier Raynaud, Knut-Andreas Lie

Abstract In this work, we review a set of consistent discretizations for second-order elliptic equations, and compare and contrast them with respect to accuracy, monotonicity, and factors affecting their computational cost (degrees of freedom, sparsity, and condition numbers). Our comparisons include the linear and nonlinear TPFA method, multipoint flux-approximation (MPFA-O), mimetic methods, and virtual element methods. We focus on incompressible flow and study the effects of deformed cell geometries and anisotropic permeability.

1 Introduction

Models of petroleum reservoirs with complex geology tend to have grids with general hexahedral or polyhedral cell geometries and tensor permeabilities. The standard two-point flux-approximation (TPFA) method is only consistent for K-orthogonal grids in which the principal directions of the permeability tensor align with vectors joining cell and face centroids[1]. Simulation models are often the result of upscaling [8], which tends to generate nonzero off-diagonal permeabilities, and as a rule, simulation grids will not be K-orthogonal, at least in some parts of the reservoir. The TPFA method is then not consistent and convergent, and will intro-

———————————————

Øystein S. Klemetsdal (e-mail: oystein.klemetsdal@sintef.no) · Olav Møyner · Xavier Raynaud · Knut-Andreas Lie
SINTEF Digital, Oslo Norway

[1] Other choices of primary pressure points are also possible, e.g., circumcenter for triangular grids.

duce grid-orientation effects that adversely affect the accuracy. Much research has therefore been devoted to develop consistent methods on non-K-orthogonal grids.

The multipoint flux-approximation (MPFA) scheme [1] accounts for transversal pressure variations by introducing auxiliary pressure points at the cell interfaces, which are coupled inside local interaction regions that together form a dual grid. MPFA methods retain the same low number of unknowns as TPFA, but have a larger stencil and can be somewhat cumbersome to implement for complex grids.

Mimetic methods [4] also introduce auxiliary pressure points to ensure consistency, which are kept as primary unknowns. An inherent free stabilization parameter gives a variety of specific schemes that reduce to other known discretizations on simple grids [14]. The main drawbacks of mimetic methods are that they use a mixed-hybrid formulation and involve significantly more unknowns than cell-centered methods. Mimetic methods have later been developed into virtual element methods (VEM) [21, 2], which constitute a uniform and flexible framework for higher-order discretizations on general polyhedral cells. MPFA, mimetic, and VEM are only conditionally monotone and may introduce nonphysical pressure oscillations. The nonlinear two-point scheme (NTPFA) [16, 18, 19] uses pressure-dependent transmissibilities to define a consistent *and monotone* method, but requires the solution of a nonlinear system of equations.

In this work, we compare the performance of these methods applied to the type of grid models encountered in real reservoir simulation using the open-source MRST software [13]. Our test cases involve deformed cell geometries and anisotropic permeabilities. The paper can therefore be seen as an update of [14] and [11]. Further comparisons can be found in, e.g., [7].

2 Consistent discretizations on polyhedral grids

For simplicity, we consider incompressible single-phase flow,

$$\nabla \cdot \mathbf{v} = q, \quad \mathbf{v} = -\mathbf{K}\nabla p, \quad \mathbf{x} \in \Omega \subset \mathbb{R}^d. \tag{1}$$

Discretized by a mesh consisting of n_c polygonal or polyhedral cells Ω_i with constant permeability $\mathbf{K}_i$ on each, the the control-volume formulation of (1) reads

$$\int_{\partial \Omega_i} \mathbf{v} \cdot \mathbf{n} \, ds = \int_{\Omega_i} q \, d\mathbf{x} = q_i. \tag{2}$$

Methods differ in the way they approximate the flux across intercell faces. Consider two neighboring cells as in Figure 1, with common interface Γ_{ij}. The normal vector $\mathbf{n}_{i,j}$ points from Ω_i to Ω_j, and similarly, $\mathbf{n}_{j,i} = -\mathbf{n}_{i,j}$. For the flux $v_{i,j}$ across Γ_{ij} in the direction of $\mathbf{n}_{i,j}$, local conservation of mass requires $v_{i,j} = -v_{j,i}$.

Discrete conservation of mass is a natural requirement, and also necessary to avoid nonphysical solutions in multiphase simulations; consistency is needed for a correct solution, typically used together with coercivity to prove convergence
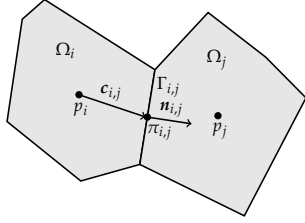
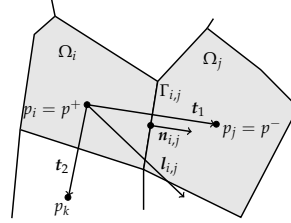**Fig. 1** Two neighboring cells and geometric quantities used to discretize the flux $v_{i,j}$.

Fig. 2 The NTPFA vector $\mathbf{l}_{i,j} = \mathbf{K}_i \mathbf{n}_{i,j}$.

[4, 19]; whereas a monotonicity is desirable to produce physically meaningful solutions with properties inherent to elliptic problems [9]. For linear discretizations, a sufficient condition for monotonicity is that the discretization produces a so-called M-matrix. Lack of coercivity may nonetheless lead to convergence breakdown, even for consistent methods [5]. We present a set of consistent discretization methods for (1), and discuss some of these properties; see Figure 3 for a schematic comparison.

Two-point flux-approximation With an auxiliary pressure point $\pi_{i,j}$ at the centroid of Γ_{ij}, we can use a one-sided finite-difference to approximate the pressure gradient in Darcy's law,

$$
v_{i,j} = \int_{\Gamma_{i,j}} \mathbf{v} \cdot \mathbf{n}_{i,j}\,\mathrm{d}s \approx |\Gamma_{i,j}| \frac{\mathbf{c}_{i,j}^T \mathbf{K}_i \mathbf{n}_{i,j}}{|\mathbf{c}_{i,j}|^2} (p_i - \pi_{i,j}) = T_{i,j}(p_i - \pi_{i,j}). \tag{3}
$$

Here, $\mathbf{K}_i$ is the constant value of $\mathbf{K}$ on Ω_i, and $T_{i,j}$ is referred to as the one-sided transmissibility. Imposing flux continuity across interfaces, $v_{ij} = v_{i,j} = -v_{j,i}$, and continuity of face pressures, $\pi_{ij} = \pi_{i,j} = \pi_{j,i}$, gives the system

$$
\sum_{j=1}^{n_c} T_{ij}(p_i - p_j) = q_i, \qquad T_{ij} = \left(T_{i,j}^{-1} + T_{j,i}^{-1}\right)^{-1}, \qquad i = 1,\dots,n_c, \tag{4}
$$

where T_{ij} is the transmissibility. If these cells do not share an interface, the transmissibility T_{ij} is zero. This yields an M-matrix, which guarantees that the method is monotone. However, the TPFA method is only consistent for K-orthogonal grids, for which a sufficient condition is that $\mathbf{K}_i \mathbf{n}_{i,j}$ is parallel to $\mathbf{c}_{i,j}$ for all cells.

Multipoint flux approximation For a consistent method, one must account for pressure gradients parallel to cell faces. MFPA-O constructs an interaction region around each grid node and defines linear basis functions for pressure inside, with pressure continuity at face centroids and flux continuity across face patches. Continuity and mass conservation gives a consistent method, with unknown cell pressures and face pressures along the *outer* boundary. This gives a denser linear system than for TPFA. However, the method is only monotone under specific conditions, and we can not expect it to be monotone for very skewed grid cells and/or severely anisotropic permeabilities [9]. See, e.g., [1, 6] for more details of MPFA schemes.
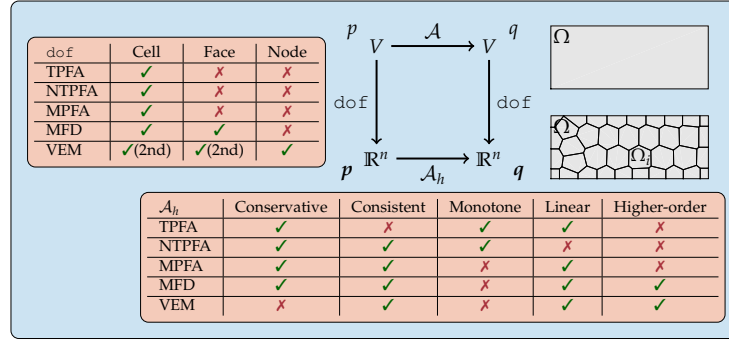
dof	Cell	Face	Node
TPFA	✓	✗	✗
NTPFA	✓	✗	✗
MPFA	✓	✗	✗
MFD	✓	✓	✗
VEM	✓(2nd)	✓(2nd)	✓

$\mathcal{A}_h$	Conservative	Consistent	Monotone	Linear	Higher-order
TPFA	✓	✗	✓	✓	✗
NTPFA	✓	✓	✓	✗	✗
MPFA	✓	✓	✗	✓	✗
MFD	✓	✓	✗	✓	✓
VEM	✗	✓	✗	✓	✓

Fig. 3 Schematic overview of key properties of the methods compared in this paper.

Nonlinear two-point flux approximation The NTPFA method [16, 18, 20] also uses additional points to estimate fluxes,

$$v_{i,j} = T_{i,j}(\mathbf{p})p_i - T_{j,i}(\mathbf{p})p_j.$$

The transmissibilities $T_{i,j}$ are positive functions that depend on one or more pressure values, giving a nonlinear method. To derive such a scheme, we consider the vector $\mathbf{l}_{i,j} = \mathbf{K}_i\mathbf{n}_{i,j}$, (see Figure 2). Whereas TPFA approximates $\mathbf{l}_{i,j}$ using only vector components normal to the interface, NTPFA uses a decomposition onto a basis of d vectors in d spatial dimensions. This is used to obtain consistent discretizations of $v_{i,j}$ and $v_{j,i}$, with v_{ij} taken as a convex combination of these. The result is a consistent and monotone two-point flux approximation, where the transmissibilities depend on pressure values not included in the two-point stencil.

Mimetic finite differences TPFA and MPFA-O can be seen as special cases of a wider family of mass-conservative schemes written in so-called *hybrid formulation*

$$\mathbf{v}_i = \mathbf{T}_i(\mathbf{e}_i p_i - \pi_i), \quad \text{in } \Omega_i.$$

Here, $\mathbf{v}_i$ is the vector of fluxes across the n_f cell faces, $\mathbf{e}_i = (1,\ldots,1)^T \in \mathbb{R}^{n_f}$, π_i is the vector of face pressures, and $\mathbf{T}_i$ is a matrix of one-sided transmissibilities. Discrete mass conservation and flux continuity is imposed through separate equations, see e.g., [14] for details. This formulation can be interpreted as a first-order mimetic finite difference method, where different choices of the inner product matrices $\mathbf{M}_i = \mathbf{T}_i^{-1}$ lead to different special cases (e.g., TPFA or MPFA-O, see [15, 14]).

The virtual element method In their present formulation, neither of the methods mentioned so far are easily extended to higher order. By using moments of the solution as degrees of freedom, it is possible to obtain a unified, higher-order framework for general polyhedral grids called the virtual element method (VEM) [21, 2]. Herein, we use this method as an example of a finite element-type discretization for

Table 1 Key characteristics of the discrete systems for the monotonicity example: number of primary unknowns (dof), number of nonzero entries in discretization matrix (nnz), average number of nonzero entries per unknown (ratio=nnz/dof), and condition number (cond).

	points for unknowns	calculation	dof	nnz	ratio	cond
TPFA	cells	$51 \cdot 51$	2601	12801	4.92	1.45e+03
NTPFA	cells	$51 \cdot 51$	2601	17208	6.62	2.83e+03
MPFA	cells + outer faces	$51^2 + 2 \cdot 4 \cdot 51$	3009	23209	7.71	1.69e+03
MFD	faces	$2 \cdot 51 \cdot 52 - 4 \cdot 51$	5100	35096	6.88	7.01e+03
VEM1	vertices	$52 \cdot 52$	2704	22704	8.40	5.08e+04
VEM2	cells + faces + vertices	$52^2 + 51^2 + 2 \cdot 51 \cdot 52$	10609	162817	15.35	1.07e+06

polyhedral grids. This formulation is not locally conservative, and the result must be postprocessed in order to be used in transport simulations. Alternatively, it is possible to use a mixed formulation [3]. We will denote first- and second-order VEM by VEM1 and VEM2, respectively.

3 Numerical experiments

All discretizations are implemented in MRST [13]. Full codes for the following two examples are available online[2], and [10] gives a more elaborate description.

Monotonicity The fundamental elliptic maximum principle of (1) implies that if there is a single source within the domain, the pressure will decrease monotonically towards the boundary. To assess deviations from monotonicity, we consider anisotropic permeability $K_x/K_y = 500$, rotated by an angle $\pi/8$, and three different meshes: 51×51 Cartesian, honeycombed PEBI, and a rotated Cartesian mesh aligned with the principal axes of **K**. We place a point source at the origin, and impose zero pressure boundary conditions. Figure 4 reports approximate solutions. All consistent methods, except NTPFA, give oscillations along the minor principal axis of **K**. Figure 5 reports fraction and magnitude of negative pressures values.

NTPFA and TPFA are monotone by construction and have no cells with negative pressure. VEM1 has the highest fraction of negative pressures, but the magnitude is lower than for MFD and MPFA. MPFA has the highest magnitude of negative pressures. VEM2 yields far better results in terms of physically meaningful pressure fields, even though the method is not guaranteed to be monotone.

Table 1 reports characteristics of the linear systems on the Cartesian mesh. MPFA has almost twice as many nonzero entries per unknown as TPFA, but similar condition number. NTPFA has a sparsity pattern similar to MPFA. MFD is less dense than for MFPA, but has three times higher condition number. VEM1 has fewer unknowns than MPFA, denser stencil, and condition number $\mathcal{O}(10)$ larger than the other. VEM2's stencil is more than three times denser than TPFA, with $\mathcal{O}(10^3)$ larger condition number. Results are similar on the rotated mesh. On the PEBI mesh, MFD and VEM are significantly denser, in particular MFD and VEM2, because the PEBI mesh has 1.5 as many faces as the Cartesian.

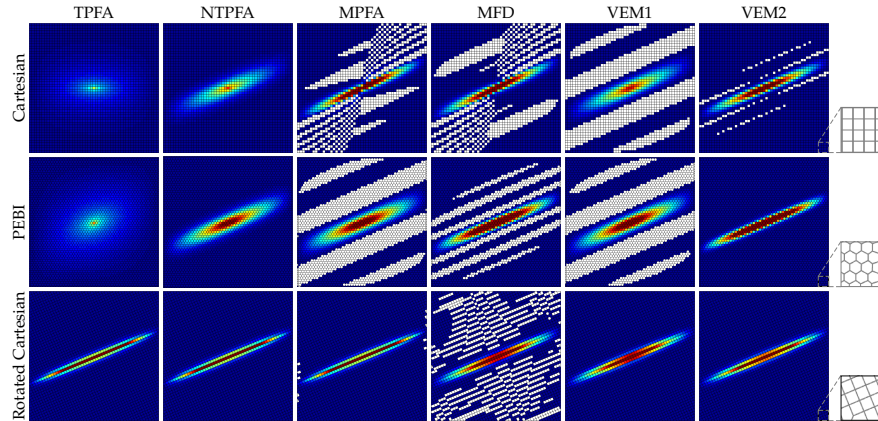[2] git@bitbucket.org:strene/compare-elliptic.git

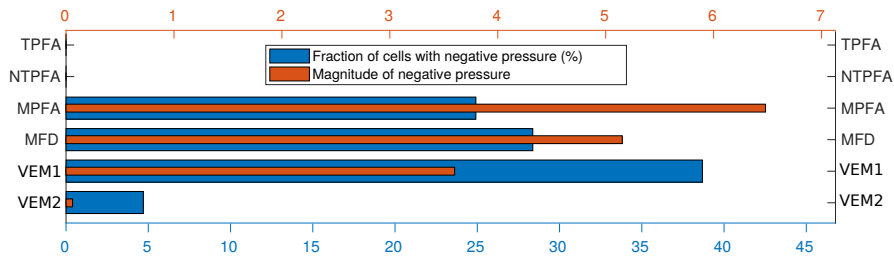**Fig. 4** Pressure solutions for the monotonicity test; white cells indicate negative pressure.

Fig. 5 Fraction and magnitude of negative pressure values for the solutions in the monotonicity test on the Cartesian mesh. Magnitude of negative pressure $= 100\sum_{p_i<0}|p_i|\big/\sum_i|p_i|$.

Fig. 6 Near-well case: **K** is log-normal, $K_x/K_y = 3$, rotated $\pi/6$ in the xy-plane. Fractures in black, topmost well-cell in red at the fracture intersection.
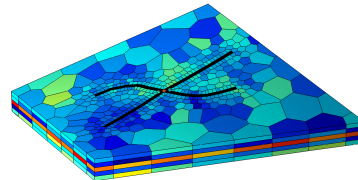
Near-well simulation Grid blocks in real field models usually represent upscaled volumes containing significant permeability variation. We consider a near-well region with a vertical well, modelled as a source injecting 1 PV over 0.1 yrs. Two fractures intersect the well, modelled as volumetric objects with a much higher permeability (Figure 6). Constant pressure is imposed the vertical sides, with no-flow top/bottom. All the consistent schemes predict similar outflow through the four vertical sides, with VEM1 deviating most (7%) from the other four. TPFA differs with as much as 20%, which is reason for serious concern, if used for upscaling.

Table 2 confirms that differences in algebraic complexity are accentuated compared to the 2D cases. VEM is *very* dense, with VEM2 having a ratio of 82.7. All methods have significantly higher condition numbers, with MFD and VEM be-

Table 2 Key characteristics of the discrete systems for the near-well example.

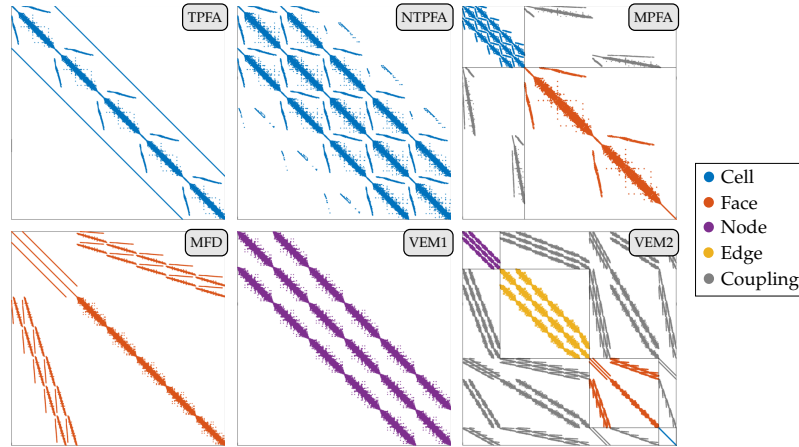|	dof	nnz	ratio	cond
TPFA	2465	19809	8.04	1.11e+04
NTPFA	2465	33608	13.63	3.26e+05
MPFA	8507	98579	11.59	6.74e+04
MFD	9658	130438	13.51	2.94e+09
VEM1	5274	170618	32.35	2.22e+11
VEM2	30173	2495409	82.70	1.44e+12

Fig. 7 Sparsity patterns from the near-well example, with different colors for each type of dof.

ing more ill-conditioned than the other methods. Figure 7 reports sparsity patterns. Since TPFA is not consistent on this grid, the converged NTPFA discretization is similar to that of MPFA instead of TPFA. VEM2 has a face-pressure block equal to MFD, and a node-pressure block equal to that of VEM1.

4 Closing remarks

The novelty herein is that we compare a large set of discretizations on the same problem, with access to complete source codes. Our experiments here and in [11] do not clearly point to one preferred method that is significantly better than the others. TPFA is inconsistent and has grid orientation effects, but is monotone and gives sparse matrices with low condition numbers. Consistent methods are convergent and reduce grid orientation effects, but have monotonicity issues and give denser and more ill-conditioned linear systems, particularly for VEM. NTPFA is monotone but requires the solution of a nonlinear system and is, in our experience, significantly less robust than e.g., mimetic methods. Our best advice is to compute representative flow solutions with more than one consistent scheme and use the results to estimate the level of error that may arise because of anisotropic permeability and skew and irregular cell geometries. For multiphase simulations, one should assess the quality of

the resulting flow fields using e.g., flow diagnostics [13]: sweep, drainage, and well-pair regions, well-allocation factors, time-of-flight, and residence time distributions. In addition, one should also investigate the number and size of the connected components in the computed flux fields, as these will affect convergence behavior of nonlinear solvers used in each time step of a multiphase simulation [17, 12].

References

1. Aavatsmark, I.: An introduction to multipoint flux approximations for quadrilateral grids. Comput. Geosci. **6**(3-4), 405–432 (2002)
2. Ahmad, B., Alsaedi, A., Brezzi, F., Marini, L.D., Russo, A.: Equivalent projectors for virtual element methods. Comput. Math. with Appl. **66**(3), 376–391 (2013)
3. Brezzi, F., Falk, R.S., Donatella Marini, L.: Basic principles of mixed virtual element methods. ESAIM Math. Model. Numer. Anal. **48**(4), 12271240 (2014)
4. Brezzi, F., Lipnikov, K., Shashkov, M.: Convergence of the mimetic finite difference method for diffusion problems on polyhedral meshes. SIAM J. Numer. Anal. **43**(5), 1872–1896 (2005)
5. Droniou, J.: Finite volume schemes for diffusion equations: introduction to and review of modern methods. Math. Mod. Meth. Appl. Sci. **24**(08), 1575–1619 (2014)
6. Edwards, M.G., Rogers, C.F.: A flux continuous scheme for the full tensor pressure equation. In: ECMOR IV-4th European Conference on the Mathematics of Oil Recovery (1994)
7. Eymard, R., et al.: 3D benchmark on discretization schemes for anisotropic diffusion problems on general grids. In: J. Fořt, et al. (eds.) Finite Volumes for Complex Applications VI Problems & Perspectives, pp. 895–930. Springer Berlin Heidelberg, Berlin, Heidelberg (2011)
8. Farmer, C.: Upscaling: a review. Int. J. Numer. Methods Fluids **40**(1-2), 63–78 (2002)
9. Keilegavlen, E., Aavatsmark, I.: Monotonicity for MPFA methods on triangular grids. Comput. Geosci. **15**(1), 3–16 (2011)
10. Klemetsdal, Ø.S.: Efficient solvers for field-scale simulation of flow and transport in porous media. Ph.D. thesis, Norwegian University of Science and Technology (2019)
11. Klemetsdal, Ø.S., et al.: Unstructured gridding and consistent discretizations for reservoirs with faults and complex wells. In: SPE Reservoir Simulation Conference (2017)
12. Klemetsdal, Ø.S., et al.: Efficient reordered nonlinear Gauss–Seidel solvers with higher order for black-oil models. Comput. Geosci. (2019)
13. Lie, K.A.: An Introduction to Reservoir Simulation Using MATLAB/GNU Octave. Cambridge University Press (2019)
14. Lie, K.A., et al.: Open-source MATLAB implementation of consistent discretisations on complex grids. Comput. Geosci. **16**(2), 297–322 (2012)
15. Lipnikov, K., Shashkov, M., Yotov, I.: Local flux mimetic finite difference methods. Numer. Math. **112**(1), 115–152 (2009)
16. Lipnikov, K., et al.: Monotone finite volume schemes for diffusion equations on unstructured triangular and shape-regular polygonal meshes. J. Comput. Phys. **227**(1), 492–512 (2007)
17. Natvig, J.R., et al.: An efficient discontinuous Galerkin method for advective transport in porous media. Adv. Water Resour. **30**(12), 2424–2438 (2007)
18. Nikitin, K., Terekhov, K., Vassilevski, Y.: A monotone nonlinear finite volume method for diffusion equations and multiphase flows. Comput. Geosci. **18**(3-4), 311–324 (2014)
19. Schneider, M., et al.: Convergence of nonlinear finite volume schemes for heterogeneous anisotropic diffusion on general meshes. J. Comput. Phys. **351**, 80–107 (2017)
20. Schneider, M., et al.: Monotone nonlinear finite-volume method for challenging grids. Comput. Geosci. **22**(2), 565–586 (2018)
21. Beirão da Veiga, L., et al.: Basic principles of virtual element methods. Math. Model. Methods Appl. Sci. **23**(01), 199–214 (2013)